Yields and Migration Distances of Reducing Equivalents in the Radiolysis of Silica Nanoparticles

Bratoljub H. Milosavljevic, Simon M. Pimblott, and Dan Meisel*

Radiation Laboratory and Department of Chemistry and Biochemistry, University of Notre Dame, Notre Dame, Indiana 46556

Received: January 16, 2004

The reduction of methyl viologen ions, MV^{2+}, adsorbed on SiO_2 nanoparticles in N_2O saturated colloidal suspensions has been studied using the pulse radiolysis technique. Reduced methyl viologen, MV^+, was produced within the electron pulse, followed by slower reactions of MV^{2+} with OH and H radicals. The fast formation of MV^+ was taken as evidence that electrons produced in the initial ionization events within the SiO_2 particles rapidly migrate to the surface and reduce the adsorbed molecules; however, yields of MV^+ as high as 6.5 radicals per 100 eV were measured, significantly exceeding common yields for ionization of less than 4.5 per 100 eV. The high yields suggest that an additional source for reduction equivalents is generated in the silica and is scavenged by the adsorbed MV^{2+} acceptor. Monte Carlo track structure calculations point to radiation-induced excitons as the scavengeable reducing species. The yield of MV^+ radicals decreases linearly with increasing particle size at a given surface coverage by MV^{2+}. This decrease in yield was attributed to a competition between electron−hole recombination within the silica bulk and scavenging of electrons at the interface. The limiting size at which no reducing equivalents arrive at the aqueous side of the interface was estimated to be $d \sim 30$ nm.

Introduction

Comparison between the irradiation of nanoparticles suspended in an aqueous phase and the irradiation of bulk solid state can provide insight into processes that cannot be obtained otherwise. This information could be particularly illuminating when studying phenomena that occur at short distances that are comparable to the size of the particle. The mean free path for migration in many materials before an electron localizes in a trap or recombines and annihilates by reacting with its counter charge carrier is of nanoscale dimensions.[1] Thus, insight into the efficiency of these processes can be gained by studying particles of similar dimensions. This topic is the subject of the present report. We study the capture of reducing equivalents, generated in SiO_2 nanoparticles, by acceptors adsorbed at the interface between the particle and an aqueous medium.

Because of the large surface-to-mass ratio in nanoparticle suspensions, the effects of adsorbates on radiolytic yields can be amplified. Indeed, several studies report the radiolytic production of molecular fragments at the aqueous interface of colloidal particles.[2−10] Some of these studies show unusual yields of radiolytic products. For example, Petrik and co-workers report unusually high molecular hydrogen yields from wet slurries of several metal oxides.[7] They attribute the large yield to scavenging of excitons by adsorbed water molecules, because of the band gap dependence of that yield and because of its correlation with thermal annihilation of charge carriers in the solid. LaVerne and co-workers, on the other hand, find more conventional yields of hydrogen from some of these oxides,[8,10] but they also report that the yield of H_2 depends on the particle size.[9] Capture of excitons at the surface of solid particles has been invoked in very early studies of radiolytic yields at solid surfaces.[3,4] The basic observation is often the same, namely relatively high yields of a product are observed, which cannot be reconciled with known limits for the yield of ionization events, and thus require another species that does not lead to ionization. In the present study, we observe high reduction yields at the interface between SiO_2 nanoparticles and water, which require a radiation-induced reducing species in addition to the electron.

The approach used in this study expands earlier studies on capture of charge carriers at the silica nanoparticle−water interface.[11] We measured the yield for adsorbate reduction in the radiolysis of colloidal silica suspensions. In addition to the high yields of reduction, particle size effects were also observed, which in turn allow an estimate of the limiting range for migration of electrons (and excitons) before they localize, recombine, and annihilate within the solid.

Experimental Section

Pulse radiolysis experiments were performed using 2−14 ns pulses of 8 MeV electrons from the Notre Dame accelerator (TB-8/16-1S linac). Details of the linac, the spectrophotometric detection setup, and the computer-controlled data acquisition and detection systems are described elsewhere.[12] Figure 1 shows the profile of a 14 ns pulse used to measure the yields described below. As can be seen in this figure, the pulse is essentially rectangular, and therefore the increase in the concentration of the hydrated electron during the pulse can be well approximated by a linear function. This significantly simplifies accurate computer simulations of the species studied. All radiolytic experiments were performed at 18 °C in a high-purity silica cell of 1 cm optical path length. The concentrations of radicals generated were in the range of 2−20 μM per pulse as determined by the thiocyanate dosimeter.[13] All solutions were deaerated by bubbling N_2 gas for 30 min immediately prior to irradiation. When necessary, the hydrated electrons were converted to hydroxyl radical by saturating the solution with N_2O.

* Corresponding author. E-mail: dani@nd.edu.

10.1021/jp049760c CCC: $27.50
Published on Web 05/08/2004

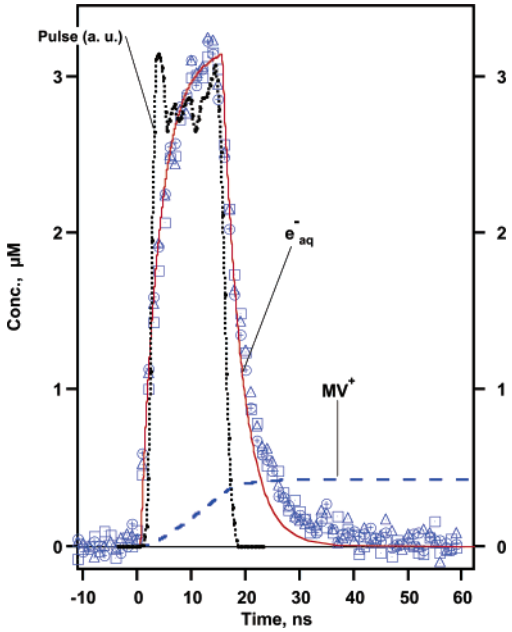

Figure 1. Pulse radiolysis experiment on 5 wt % dialyzed 7 nm SiO_2 particles and 10 mM MV^{2+} aqueous solution saturated with N_2O. Concentration of e_{aq}^- calculated from absorbance at 785 nm (data points) and computer simulation of the same experiment (solid curve). Parameters used to simulate those data are given in the text. Dashed curve corresponds to the calculated MV^+ concentration produced in the reaction with e_{aq}^-. Dotted curve is the current profile of the 14 ns electron pulse.

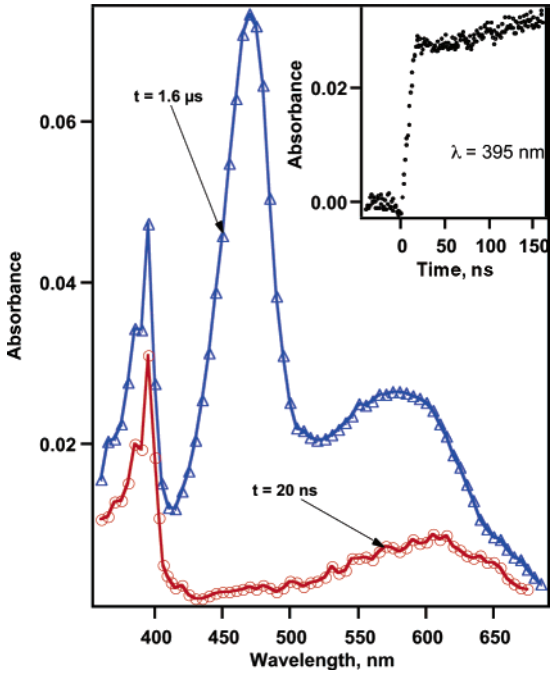

Figure 2. Transient absorption spectra of irradiated MV^{2+} and SiO_2 colloidal suspensions taken at the end of 14 ns pulses (circles) and at 1.6 μs after the pulse (triangles). Experimental conditions: $[SiO_2] = 5$ wt %, $[MV^{2+}] = 3$ mM, N_2O saturated solutions. Insert shows the trace corresponding to MV^+ absorbance at 395 nm.

Methyl viologen dichloride hydrate salt and all other chemicals used were of the highest purity commercially available and were used as received. Three types of Ludox colloidal silica dispersions (Aldrich) were used: SM-30 (30 wt % SiO_2 in H_2O, pH 10.2, specific surface area = 345 $m^2\ g^{-1}$), HS-40 (40 wt % SiO_2 in H_2O, pH 9.7, specific surface area = 220 $m^2\ g^{-1}$), and TM-50 (50 wt % SiO_2 in H_2O, pH 10.2, specific surface area = 140 $m^2\ g^{-1}$). Assuming the density for the particles is 2.3 g cm^{-3}, identical to that for bulk silica, the surface areas translate to radii of 3.8, 5.9, and 9.3 nm, respectively. These values are close, but not identical, to the sizes provided by the manufacturer (r = 3.5, 6, and 11 nm, respectively). Surface areas were determined using the BET method on the dried suspensions with nitrogen gas as adsorbent. Soluble impurities in the commercial suspensions were removed by dialysis against aqueous NaOH solution at pH 10 for several days. The half-life of e_{aq}^- in the deaerated suspensions following the dialysis was $\geq 7 \times 10^{-6}$ s, essentially the value observed in N_2 saturated distilled water. All experiments were conducted at pH 10.0 ± 0.2.

Results and Discussion

Surface versus Bulk Water Reactions of Methyl Viologen. Figure 2 shows the transient absorption spectra of the species produced in the pulse radiolysis of N_2O saturated 5 wt % SiO_2 colloidal solution containing 3 mM MV^{2+}. Open circles correspond to the spectrum taken at 20 ns immediately after 14 ns electron pulse. The triangles in Figure 2 correspond to the spectrum taken at 1.6 μs after the pulse. The insert shows the kinetics of the changes in absorbance on the short time scale. Two distinct processes can be observed in the insert: an instantaneous formation within the pulse and a slower formation. From the characteristics of the spectrum recorded at the end of the electron pulse (absorption maxima at 395 and 600 nm), one concludes that the fast process, which takes place within the duration of electron pulse, is reduction of MV^{2+}. The spectrum of the intermediates at the end of the slower process is attributed to the products of the reactions of MV^2 with OH and H radicals.[14,15] The latter reactions will not be considered any further in the present report.

The MV^+ radical observed in the pulse radiolysis experiments can be produced either at the SiO_2 surface or in the aqueous phase via two completely different processes; therefore, the reduction process of MV^{2+} needs to be scrutinized first. We have recently shown that the adsorption−desorption equilibrium constant of MV^{2+} at SiO_2 surfaces at pH 10 is $K = (4.7 \pm 0.3) \times 10^5\ M^{-1}$, and is independent of particle size.[16] Such a large equilibrium constant implies that nearly all MV^{2+} is adsorbed on the particles, and thus the reduction takes place at the SiO_2 surface. Free MV^{2+} in the aqueous phase cannot be reduced on this time scale. Two processes may then lead to the observed "instantaneous" formation of MV^+. This reduction may occur either by electrons generated in the particles or by hydrated electrons from the aqueous phase. It is possible that a fraction of e_{aq}^- may react with MV^{2+} adsorbed on the SiO_2 surface despite the fast reaction with N_2O. Therefore, the two parallel reactions

$$e_{aq}^- + N_2O\ (+H_2O) \rightarrow N_2 + OH + (OH^-) \qquad (1)$$

and

$$e_{aq}^- + MV^{2+}{}_{ads} \rightarrow MV^{+}{}_{ads} \qquad (2)$$

may be in competition. Any contribution from the reaction of bulk e_{aq}^- with adsorbed MV^{2+} to the absorbance by MV^+ at the end of the pulse needs to be subtracted from the observed one.

The correction for the $MV^+{}_{ads}$ yield originating from reaction 2 was performed in the following manner: Prior to each measurement of the yield of MV^+, the suspension was first saturated with N_2 and the decay of the hydrated electron at 785

nm was measured. This measurement provided the value of the pseudo-first-order rate constant for $e_{aq}^- + MV^+_{ads}$, reaction 2. From the previously determined values[17] of the rate constant of reaction 1 at 20 and 25 °C, and the high (negative) N_2O solubility coefficient (~3% per °C), the pseudo-first-order decay rate constant for e_{aq}^- with N_2O in saturated aqueous solution was estimated to be 2.7×10^8 s^{-1} at 18 °C. These values were used to correct for the contribution of reaction 2 to the "instantaneous" generation of MV^+.

Figure 1 shows experimental results and computer simulations of the concentration profile of e_{aq}^- and MV^+ in a pulse radiolysis experiment performed on dialyzed 5 wt % silica aqueous suspension of particles of 7 nm size containing 10 mM MV^{2+} and saturated with N_2O. The formation and decay of e_{aq}^- were measured at 785 nm (data points in Figure 1). Computer simulation of the same experiment (solid line) was obtained using the following parameters: dose = 40 Gy; $k(N_2O + e_{aq}^-) \times [N_2O] = 2.7 \times 10^8$ s^{-1}; $k(MV^{2+} + e_{aq}^-) \times [MV^{2+}] = 8.8 \times 10^6$ s^{-1}; extinction coefficient of e_{aq}^- at 785 nm is 1.6×10^4 M^{-1} cm^{-1}. The dashed curve corresponds to the calculated MV^+ concentration produced in the reaction with e_{aq}^- from the aqueous phase. The dotted curve in Figure 1 shows the time profile of the current of a 14 ns electron pulse. The rectangular pulse shape allows a linear approximation for the buildup of the electron concentration within the pulse to be used in the computer simulations. A yield of $G(e_{aq}^-) = 3.4$ radicals per 100 eV was used in the simulations as the scavenger capacity of the experiment was $\sim 3 \times 10^8$ s^{-1}.[18] The calculated value for the MV^+ produced in the reaction of e_{aq}^- was subtracted from the total MV^+ yields measured at the end of the pulse at 395 nm. This corrected value of $[MV^+]$ at the end of the pulse is taken to represent the amount of reducing equivalents that reach the surface from the bulk of the particle.

Yields of MV^{2+} Reduction at the Interface. The initial ionization event in the silica particle generates an electron−hole pair:

$$SiO_2 \rightsquigarrow e^- + h^+ \qquad (3)$$

The charge carriers can recombine via an exciton state and relax to the ground state in either radiative or nonradiative processes:

$$e^- + h^+ \rightarrow (\text{exciton}) \rightarrow SiO_2 + \Delta Q \qquad (4)$$

It has been suggested that excitons in hydroxylated silica react with the surface hydroxyl groups:[19]

$$(\text{exciton}) + \equiv Si-OH \rightarrow \equiv Si-O + H \qquad (4A)$$

Both electrons and holes can be scavenged by adsorbates, A, at the surface:

$$h^+ + A \rightarrow A^+ \qquad (5)$$

$$e^- + A \rightarrow A^- \qquad (6)$$

In competition with reactions 4−6, both the holes and electrons may localize at a trap either on the surface or in the bulk. However, depending on the redox potential of the adsorbate and the energy level of the trapped carrier, both carriers may still react with surface species. It is now well established that the electrons can cross the interface of a silica nanoparticle in water to produce hydrated electrons:[20]

$$e^- + nH_2O \rightarrow e_{aq}^- \qquad (7)$$

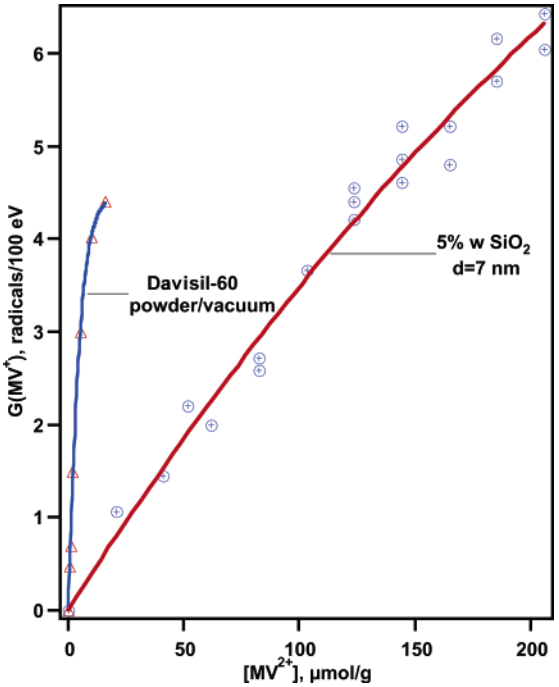

Figure 3. Yield of MV^+ at various MV^{2+} loadings on SiO_2 colloidal 7 nm particles (circles). $[MV^{2+}]$ is expressed in micromoles per gram of silica. Triangles represent data taken from ref 22, insert in Figure 11. See text for details.

Holes, on the other hand, do not cross the interface.[12] The dominant reaction of the above reactions depends on the specific experimental conditions. It is clear from Figure 2 that little, if any, oxidation of MV^{2+} occurs immediately after the pulse.

Figure 3 shows the yield of electron scavenging by MV^{2+} in 5 wt % dialyzed colloidal SiO_2 suspension of 7 nm particles saturated with N_2O immediately following the pulse. Thomas and co-workers[22] studied radiation-induced reduction of methyl viologen adsorbed on dry powders of porous silica particles (Davisil; grade 635, 100−200 mesh, pore size = 6 nm, surface area = 480 m^2 g^{-1}, pore volume = 0.75 cm^3 g^{-1}). Yields of electron scavenging by MV^{2+} were measured in a vacuum also using the pulse radiolysis technique. Their results (taken from Figure 11 in ref 22) significantly differ from those measured here in aqueous colloidal solutions even though the specific surface area is similar (from the specific surface area given above one calculates equivalent particles of $r = 2.7$ nm). The initial slope of the curve obtained in the solid−vacuum system is 25 times larger than that corresponding to the colloidal solution. The difference observed could be attributed to the localization of electrons in the aqueous phase surrounding the SiO_2 particles that leads to the production of e_{aq}^-. Furthermore, the powder experiments with SiO_2 were conducted under vacuum. In such an environment, the electrons can cross the interface several times and reenter the solid particles until they thermalize, localize, or are scavenged by MV^{2+}. In the suspension, a thermalized electron that exits a parent particle would not be able to enter another particle before it hydrates to give e_{aq}^-.

The effect of particle size on the efficiency of the scavenging of electrons (from within the particles) was determined for the three particle sizes: 7, 12, and 22 nm in diameter. Figure 4 compares the yields as a function of percentage of surface loading by MV^{2+} for the various sizes. As can be seen in Figure 4, the yield of electrons scavenged at the surface decreases with increasing particle size for a given surface coverage. Surface coverage is chosen as an independent variable, because it

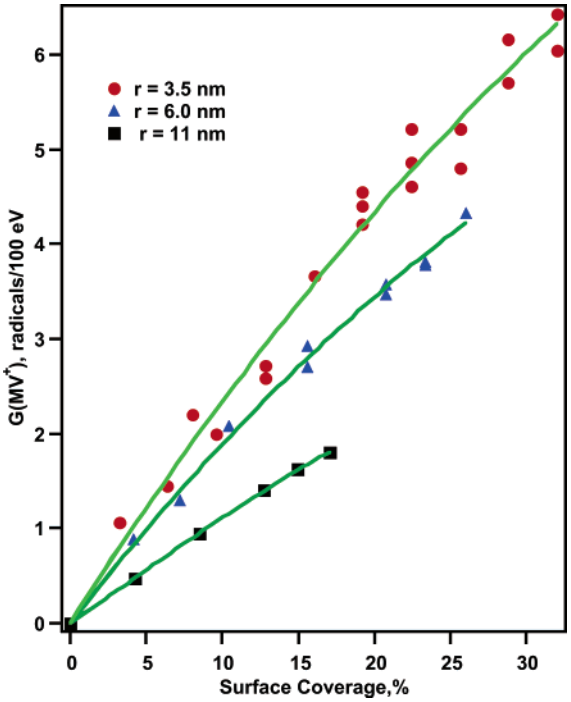

Figure 4. Yield of MV^+ at the surface of silica particles in the reaction with electrons produced inside the particles for three particle sizes. For calculating the percentage of surface loading, the cross section of one MV^{2+} molecule is assumed to be 1 nm^2. Experimental conditions: 5 wt % of 7 nm SiO_2 particles, pH 10, N_2O saturated, 14 ns pulse, dose $\cong$ 40 Gy.

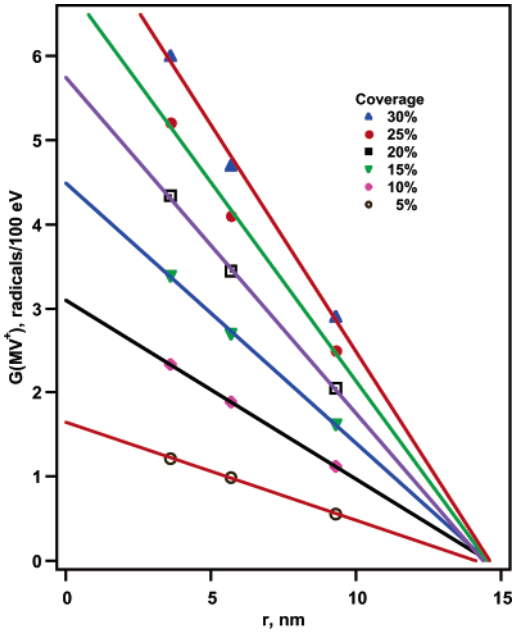

Figure 5. Dependence of the yield of instantaneous MV^+ on particle radii at various surface coverages taken from Figure 4. Some values for high coverages and large particles were extrapolated estimates.

accounts for both the change in number of adsorbed molecules per particle and the corresponding change in the surface area per particle. Thus, it can be directly related to the probability of scavenging the exiting electrons. The largest number of MV^{2+} molecules that can adsorb on the particles used in the present study has recently been determined.[16] It corresponds to 0.61 $\pm$ 0.03 molecule nm^{-2} and is essentially independent of particle size. However, no information is available to indicate the surface density of scavengers required for complete scavenging of the electrons. Therefore, in calculating the complete coverage of the particle we used 1 molecule nm^{-2}, which is a value close to the van der Waals cross section of a flat MV^{2+}. The results of Figure 4 show no saturation in the yield at high coverage, and thus shed no light on this question.

The yield of "instantaneous" MV^+ is plotted versus the corresponding particle radius in Figure 5. A linear relation is found for the limited data points available. The observed decrease of yield with increasing size can be rationalized as resulting from the increased competition from electron−hole recombination and from charge carriers trapping within the silica bulk upon increasing the size. Interestingly, on extrapolation of the straight lines obtained for various surface coverage down to a yield of $G = 0$ molecules per 100 eV, a common limiting value of $r = 15$ nm is obtained that is independent of coverage (Figure 5). This observation is interpreted to indicate that no reduction equivalents (electrons or excitons) reach the surface when the particle radius is greater than 15 nm. Of course, even in very large particles some secondary electrons are randomly generated at short distances from the particle surface and, therefore, may have high escape probability. However, this "skin effect" in large particles is apparently negligible. Hydrogen generation data obtained in the radiolysis of aqueous silica suspensions and slurries support the above conclusion. LaVerne et al.[9] found that the production of H_2 in the radiolysis of slurries of large SiO_2 particles (8.1 m^2 g^{-1}, $r \cong 160$ nm) is virtually identical to that in water alone; however, the yield in aqueous slurries of small SiO_2 particles (312 m^2 g^{-1}, $r \cong 8$ nm) is nearly double the H_2 production from water.

Finally, the highest MV^+ yield that was observed in Figure 4 is 6.5 radicals per 100 eV, significantly higher than the limiting yield of electrons at early times. This limiting yield is commonly accepted to be $\leq$4.5 radicals per 100 eV.[23] Several sources for the large yield were considered. Localization of holes on surface hydroxide groups, reaction 4A, can contribute to the high yield of MV^+. The production of an H atom in the vicinity of the particle's surface may lead to its rapid addition to MV^{2+}. The spectrum of the H-adduct is similar to that of MV^+.[14,15] Direct reduction by excitons can also lead to additional yield of instantaneous MV^+. Such a reduction reaction was invoked in the early work of Sagert and Robinson.[4] In the latter work, very high yields of N_2 (up to $G = 7$ molecules per 100 eV) were obtained upon radiolysis of N_2O adsorbed at zirconia surfaces. These high yields were attributed to the capture of excitons by the adsorbate. In the present case, the capture of an exciton may occur via a dissociative electron transfer to the adsorbed MV^{2+} or via the formation of an excited MV^{2+}. Either process would produce MV^+. Excited methyl viologen is believed to be a very powerful oxidant; from the fluorescence emission maximum and the ground state, its redox potential was estimated to be $E^\circ = 3.65$ V.[24] Indeed, Thomas and co-workers reported that UV photoexcitation of MV^{2+} adsorbed on silica surfaces produces the radical cation MV^+.[25] In the following section we show that track structure simulations predict yields of ionization and excitation similar to those observed above upon irradiation of silica particles.

Track Structure Calculations. Monte Carlo track structure simulations were performed to estimate the yields of ionization and excitation events produced by the irradiation of silica with energetic electrons. The calculations were made using the methodology detailed in refs 26 and 27, employing an energy-dependent inelastic collision cross section, $\sigma_{in}(E)$, appropriate for amorphous silica. Briefly, the methodology is as follows: the attenuation of an energetic electron and its daughter secondary electrons are modeled collision-to-collision, with the

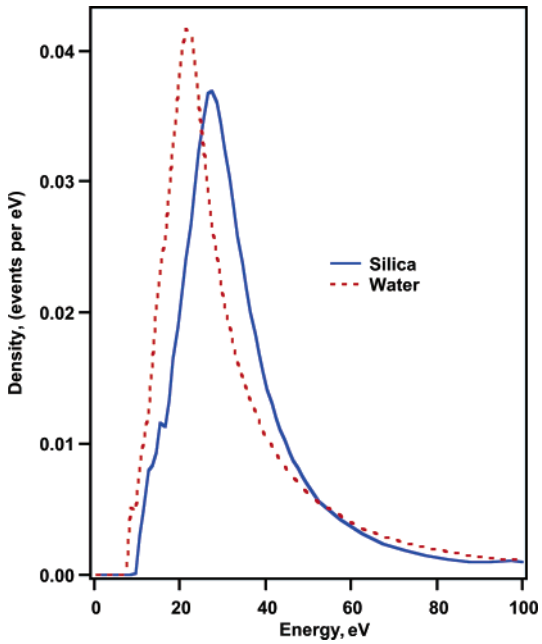

Figure 6. Density of energy-transfer events for the complete attenuation of electrons of initial 1 MeV energy.

separation between events determined by sampling from a Poisson distribution with a mean free path of $(\rho\sigma_{in}(E))^{-1}$, where ρ is the density of amorphous silica, 2.3 g cm^{-3}. The energy loss cross section, $\sigma_{in}(E)$, was calculated from the differential dipole oscillator strength distribution for silica, $f(E)$,[28] using the approach of Ashley[29] and of Green and co-workers.[30] The amount of energy transferred from the primary electron to the excited molecular electron in a collision, ΔE, is evaluated by inversion of the ratio of the cumulative inelastic collision cross section, $\sigma_{in}(\Delta E,E)$ to $\sigma_{in}(E)$, where the cumulative cross section for the maximum possible energy loss, ΔE_{max}, is $\sigma_{in}(\Delta E_{max},E)$ and is equal to $\sigma_{in}(E)$. The nature of the collision, i.e., whether the energy transfer event results in an ionization or an electronic excitation, is determined by the magnitude of ΔE. If $E_{min} < \Delta E < I_P$ then electronic excitation is assumed to occur, while if $\Delta E > I_P$ then ionization is assumed, where E_{min} and I_P are the appearance energy of $f(E)$, ~7 eV, and the vertical ionization potential for silica, ~9 eV, respectively. The simulation of the complete attenuation of a primary electron and its daughters to an energy of about 7 eV gives the yields of ionization and excitation for one track, and realization of many tracks gives average yields appropriate for energetic electron radiolysis.

The ionization and excitation yields for amorphous silica obtained by the simulation of 10^4 different tracks are 4.11 ± 0.01 and 2.19 ± 0.01 per 100 eV of energy transferred, respectively. The ionization yield obtained for silica is similar to that obtained both from pulse radiolysis experiments and calculations for liquid water; however, the yield of electronic excitation events in silica is significantly larger than that observed in water. Excitation yields in water were calculated to be less than 1.0 per 100 eV. The sum of the yields of ionization and excitation in silica is similar, perhaps slightly smaller than, the "instantaneous" yield of MV^+ observed in the pulse radiolysis experiments reported above. Detailed examination of the distribution of energy loss events reveals considerable differences between silica and water. Figure 6 shows the density of events (sum of both ionizations and excitations) in the 0−100 eV interval for the complete attenuation of electrons of initial 1 MeV energy. The most probable energy losses are at 27 and 22 eV in silica and water, respectively, while the mean energy losses are 87 and 64 eV. Clearly, there is a significant shift of energy losses to higher energy in silica compared to water, which will increase the size of the typical radiation produced spur. Thus, it is conceivable that the limiting value of 15 nm estimated for the distance above which no electrons (excitons) escape into the aqueous phase simply reflects the initial size of the spur in silica. However, the simulations also suggest that an in-depth stochastic analysis of the kinetics of the mixed phase system, including interfacial effects, is necessary to determine the significance of these sizes.

Conclusion

Electrons produced in the radiolysis of colloidal silica particles reach the surface and are capable of reducing the adsorbed MV^{2+}. Yields of up to 6.5 radicals per 100 eV were measured, which indicates that reducing equivalents, other than electrons, are involved. A possible source is energy or charge transfer from exciton states. Track structure calculations of the sum of yields of ionization and of exciton formation yield a similar value. These calculations support exciton formation as an additional source for reducing equivalents. They also indicate that the observed yield of reduced radicals is near the limiting value. The effect of particle size on MV^{2+} reduction by electrons from within the particles was measured in the range from 7 to 22 nm. The efficiency of scavenging the electrons decreases with increasing particle size due to the increased fraction of charge recombination and trapping that occurs in the larger particles. It is estimated that essentially no electrons (and excitons) will reach the surface of particles larger than 30 nm in diameter.

Acknowledgment. Support by the US Department of Energy, Office of Basic Energy Sciences, is gratefully acknowledged. This is Contribution No. NDRL 4502 from the Notre Dame Radiation Laboratory.

References and Notes

(1) Grigoriev, E. I.; Trakhtenberg, L. I. *Radiation Chemical Processes in Solid Phase. Theory and Application*; CRC Press: Boca Raton, FL, 1996.
(2) Thomas, J. K. *Chem. Rev.* **1993**, *93*, 301.
(3) Rabe, J. G.; Rabe, B.; Allen, A. O. *J. Phys Chem.* **1966**, *70*, 1098.
(4) Sagert, N. H.; Robinson, R. W. *Can. J. Chem.* **1968**, *46*, 2075.
(5) Ogura, H.; Hinata, M.; Nakazato, C.; Kondo, M.; Sawai, T. *J. Nucl. Sci. Technol.* **1978**, *15*, 433.
(6) Maeng, K. S.; Brown, G. R.; Trudel, G. J.; St-Pierre, L. E. *Can. J. Chem.* **1983**, *61*, 729.
(7) Petrik, N. G.; Alexandrov, A. B.; Vall, A. I. *J. Phys. Chem. B* **2001**, *105*, 5935.
(8) LaVerne, J. A.; Tandon, L. *J. Phys. Chem. B* **2002**, *106*, 380
(9) LaVerne, J. A.; Tonnies, S. E. *J. Phys. Chem. B* **2003**, *107*, 7277.
(10) LaVerne, J. A.; Tandon, L. *J. Phys. Chem. B* **2003**, *107*, 13623.
(11) Schatz, T.; Cook, A. R.; Meisel, D. *J. Phys. Chem. B* **1999**, *103*, 10209.
(12) Hug, G. L.; Wang, G. L.; Schoneich, C.; Jiang, P.-Y.; Fessenden, R. *Radiat. Phys. Chem.* **1999**, *54*, 559.
(13) Buxton, G. V.; Stuart, C. R. *J. Chem. Soc., Faraday Trans.* **1995**, *91*, 279.
(14) (a) Solar, S.; Solar, W.; Getoff, N.; Holcman, J.; Sehested, K. *J. Chem. Soc., Faraday Trans. 1* **1984**, *80*, 2929. (b) Solar, S.; Solar, W.; Getoff, N.; Holcman, J.; Sehested, K. *J. Chem. Soc., Faraday Trans. 1* **1985**, *81*, 1101.
(15) Das, T. N.; Ghanty, T. K.; Pal, H. *J. Phys. Chem. A* **2003**, *107*, 5998.
(16) Milosavljevic, B. H.; Meisel, D. *J. Phys. Chem. B* **2004**, *108*, 1827.
(17) Janata, E.; Schuler, R. H. *J. Phys. Chem.* **1982**, *86*, 2078.
(18) Bartels, D. M.; Gosztola, D.; Jonah, C. D. *J. Phys. Chem. A* **2001**, *105*, 8069.
(19) Shkrob, I. A.; Trifunac, A. D. *J. Chem. Phys.* **1997**, *107*, 2374.
(20) Schatz, T.; Cook, A. R.; Meisel, D. *J. Phys. Chem. B* **1998**, *102*, 7225.

(21) Dimitrijevic, N. M.; Henglein, A.; Meisel, D. *J. Phys. Chem. B* **1999**, *103*, 7073.
(22) Zhang, G.; Mao, Y.; Thomas, J. K. *J. Phys. Chem. B* **1997**, *101*, 7100.
(23) Warman, J. M. The Dynamics of Electrons and Ions in Non-Polar Liquids. In *The Study of Fast Processes and Transient Species by Electron Pulse Radiolysis*; Baxendale, J. H., Busi, F., Eds.; NATO Advanced Study Institute Series C86; Reidel: Dordrecht, Holland, 1982; p 433.
(24) Peon, J.; Tan, X.; Hoerner, J. D.; Xia, C.; Luk, Y. F.; Kohler, B. *J. Phys. Chem. A* **2001**, *105*, 5768.
(25) Mao, Y.; Breen, N. E.; Thomas, J. K. *J. Phys. Chem.* **1995**, *99*, 9909.
(26) Pimblott, S. M.; LaVerne, J. A.; Mozumder, A. *J. Phys. Chem.* **1996**, *100*, 8595.
(27) LaVerne, J. A.; Pimblott, S. M. *J. Phys. Chem. A* **1997**, *101*, 4504.
(28) Philipp, H. R. *Solid State Commun.* **1966**, *4*, 73.
(29) Ashley, J. C. *J. Electron Spectrosc. Relat. Phenom.* **1988**, *46*, 199.
(30) Pimblott, S. M.; LaVerne, J. A.; Mozumder, A.; Green, N. J. B. *J. Phys. Chem.* **1990**, *94*, 488.